Biofunctional ZnO Nanorod Arrays Grown on Flexible Substrates

Ting-Yu Liu, Hung-Chou Liao, Chin-Ching Lin, Shang-Hsiu Hu, and San-Yuan Chen*

Department of Materials Sciences and Engineering, National Chiao Tung University, Hsinchu, Taiwan, 300, ROC

Received August 30, 2005. In Final Form: April 7, 2006

A square pattern of thioctic acid self-assembled ZnO nanorod arrays was grown on a large 4-in. thermoplastic polyurethane (TPU) flexible substrate via an in situ soluthermal process at low temperature (348 K). With the addition of dimercaptosuccinic acid (DMSA), the surface chemistry forms a disordered ZnO phase, and the morphology of the ZnO−DMSA nanorods changes with various DMSA addition times. As evidenced by the $Zn_{2p3/2}$, C_{1s}, O_{1s}, S_{2p}, and N-1s scans of X-ray photoelectron spectroscopy (XPS) and X-ray diffraction (XRD), DMSA and proteins were conjugated on the single crystalline ZnO nanorods. The photoluminescence (PL) spectra indicated that the optical properties of ZnO nanorod arrays were changed while the DMSA was inserted, and proteins were conjugated. Furthermore, a control test found that the ZnO nanorods show a significant improvement in sensitive characterization over the ZnO film. As another proteins (e.g., human serum albumin, HSA) were bound onto the ZnO−bovine serum albumin (BSA) nanorod arrays, an enhanced ultraviolet emission intensity was detected. On the basis of these results, one might be expected to conjugate specific biomolecules on the biofunctional ZnO nanorod arrays to detect the complementary biomolecules by PL detecting.

1. Introduction

Recently, several researchers have reported on utilizing luminescent semiconductor quantum dots (QDs), such as CdSe and CdTe, to bind biomolecules for ultrasensitive nonisotopic detection.[1−5] Moreover, considerable progress has already been made regarding the functionalization of carbon nanotubes with proteins through bioconjugation.[6−12] Studies to integrate nanomaterials with bioconjugated biomolecules for biological applications have been reported in the literature.[13−15] Nanorods and nanowires have been considered to be promising building blocks for the miniaturization of electronic and photonic devices and biological sensors. However, studies on using nanorods for biological detecting purpose are rarely reported.

Zinc oxide (ZnO) is a key electronic and photonic material and is particularly promising in nanodevice applications because of its wide direct band gap of 3.37 eV and large exciton binding energy of 60 meV,[16] and it can be grown on selected patterned substrates, as demonstrated in an earlier publication.[17] Additionally, ZnO nanostructures have novel applications in optoelectronics, sensors, transducers, and biomedical devices.[18] Recently, several groups applied ZnO nanoparticles as seeds for the growth of large-scale and well-oriented ZnO nanorods on silica substrates.[19,20] However, it is more significant to synthesize one-dimensional (1D) nanoscale materials on organic substrates, such as polyimide (PI), polycarbonate (PC), and thermoplastic polyurethane (TPU), for optoelectronic and biomedical applications.

Zhang et al.[21] reported the immobilization of uricase by electrostatic binding on ZnO nanorods for a uric acid biosensor because it is very stable in suntan lotion. Although the idea for designing this biosensor is promising, electrostatic binding with ZnO and uricase is not stable. To solve this problem, dimercaptosuccinic acid (DMSA) has been used as a metal chelating agent to combine ZnO and proteins because DMSA can form strong complexes[22,23] and is a "nontoxic" chemical agent used in the treatment of arsenic and mercury poisoning in humans.[24] Furthermore, to date, DMSA has also been applied in Au,[25] maghemite nanoparticles,[22] CdSe−ZnS,[26] and Fe_2O_3 beads−CdSe/ZnS QD core−shell particles[27] to immobilize proteins, enzymes, DNA, or antibodies for cell separation. However,

* Corresponding author. Tel: +886-3-5731818. Fax: +886-3-5725490. E-mail address: sychen@cc.nctu.edu.tw.

(1) Willard, D. M.; Carillo, L. L.; Jung, J.; Orden, A. V. *Nano Lett.* **2001**, *1*, 469.
(2) Kagan, C. R.; Murray, C. B.; Nirmal, M.; Bawendi, M. G. *Phys. Rev. Lett.* **1996**, *76*, 1517.
(3) Kagan, C. R.; Murray, C. B.; Bawendi, M. G. *Phys. Rev. B* **1996**, *54*, 8633.
(4) Finlayson, C. E.; Ginger, D. S.; Greenham, N. C. *Chem. Phys. Lett.* **2001**, *338*, 83.
(5) Mamedova, N. N.; Kotov, N. A.; Rogach, A. L.; Studer, J. *Nano Lett.* **2001**, *1*, 281.
(6) Wang, S. G.; Wang, R.; Sellin, P. J.; Zhang, Q. *Biochem. Biophys. Res. Commun.* **2004**, *325*, 1433.
(7) Wang, Y.; Tang, Z.; Tan, S.; Kotov, N. A. *Nano Lett.* **2005**, *5*, 243.
(8) Gooding, J. J.; Wibowo, R.; Liu, J.; Yang, W.; Losic, D.; Orbons, S.; Mearns, F. J.; Shapter, J. G.; Hibbert, D. B. *J. Am. Chem. Soc.* **2003**, *125*, 9006.
(9) Huang, W.; Taylor, S.; Fu, K.; Lin, Y.; Zhang, D.; Hanks, T. W.; Rao, A. M.; Sun, Y. P. *Nano Lett.* **2002**, *2*, 311.
(10) Wohlstadter, J. N.; Wilbur, J. L.; Sigal, G. B.; Biebuyck, H. A.; Billadeau, M. A.; Dong, L.; Fischer, A. B.; Gudibande, S. R.; Jameison, S. H.; Kenten, J. H.; Leginus, J.; Leland, J. K.; Massey, R. J.; Wohlstadter, S. *J. Adv. Mater.* **2003**, *15*, 1184.
(11) Keren, K.; Berman, R. S.; Buchstab, E.; Sivan, U.; Braun, E. *Science* **2003**, *302*, 1380.
(12) Chopra, N.; Majumder, M.; Hinds, B. *J. Adv. Funct. Mater.* **2005**, *15*, 858.
(13) Flechsig, G. U.; Peter, J.; Hartwich, G.; Wang, J.; Gründler, P. *Langmuir* **2005**, *21*, 7848.
(14) Nakao, H.; Hayashi, H.; Iwata, F.; Karasawa, H.; Hirano, K.; Sugiyama, S.; Ohtani, T. *Langmuir* **2005**, *21*, 7945.
(15) Grinberg, S.; Linder, C.; Kolot, V.; Waner, T.; Wiesman, Z.; Shaubi, E.; Heldman, E. *Langmuir* **2005**, *21*, 7638.
(16) Xiong, L.; Shi, J.; Gu, J.; Li, L.; Shen, W.; Hua, Z. *Solid State Sci.* **2004**, *6*, 1341.
(17) Hsiao, C. S.; Chen, H. P.; Chen, S. Y.; Liou, S. C. *J. Vac. Sci. Technol., B* **2006**, *24* (1), 288.
(18) Wang, Z. L. *J. Phys. Condens. Matter.* **2004**, *16*, 829.
(19) Tina, A. R.; Voigt, J. A.; Liu, J.; Mckenzie, B.; Mcdermott, M. J.; Rodriguez, M. A.; Konishi, H.; Xu, H. *Nat. Mater.* **2003**, *2*, 821.
(20) Choy, J. H.; Jang, E. S.; Won, J. H.; Chung, J. H.; Kim, Y. W. *Adv. Mater.* **2003**, *15*, 1911.
(21) Zhang, F.; Wang, X.; Ai, S.; Sun, Z.; Wan, Q.; Zhu, Z.; Xian, Y.; Jin, L.; Yamamoto, K. *Anal. Chim. Acta* **2004**, *519*, 155.
(22) Fauconnier, N.; Pons, J. N.; Roger, J.; Bee, A. *J. Colloid Interface Sci.* **1997**, 194, 427.
(23) Martcll, A. E. *Inorg. Chem.* **1965**, *4*, 378.
(24) Aascth, J. *Hum. Toxicol.* **1983**, *2*, 257.
(25) Cheng, Q.; Anna, B. T. *Anal. Chem.* **1996**, *68*, 4180.
(26) Chan, W. C. W.; Nie, S. *Science* **1998**, *281*, 2016.
(27) Wang, D.; He, J.; Rosenzweig, N.; Rosenzweig, Z. *Nano Lett.* **2004**, *4*, 409.

10.1021/la052363o CCC: $33.50
Published on Web 05/23/2006

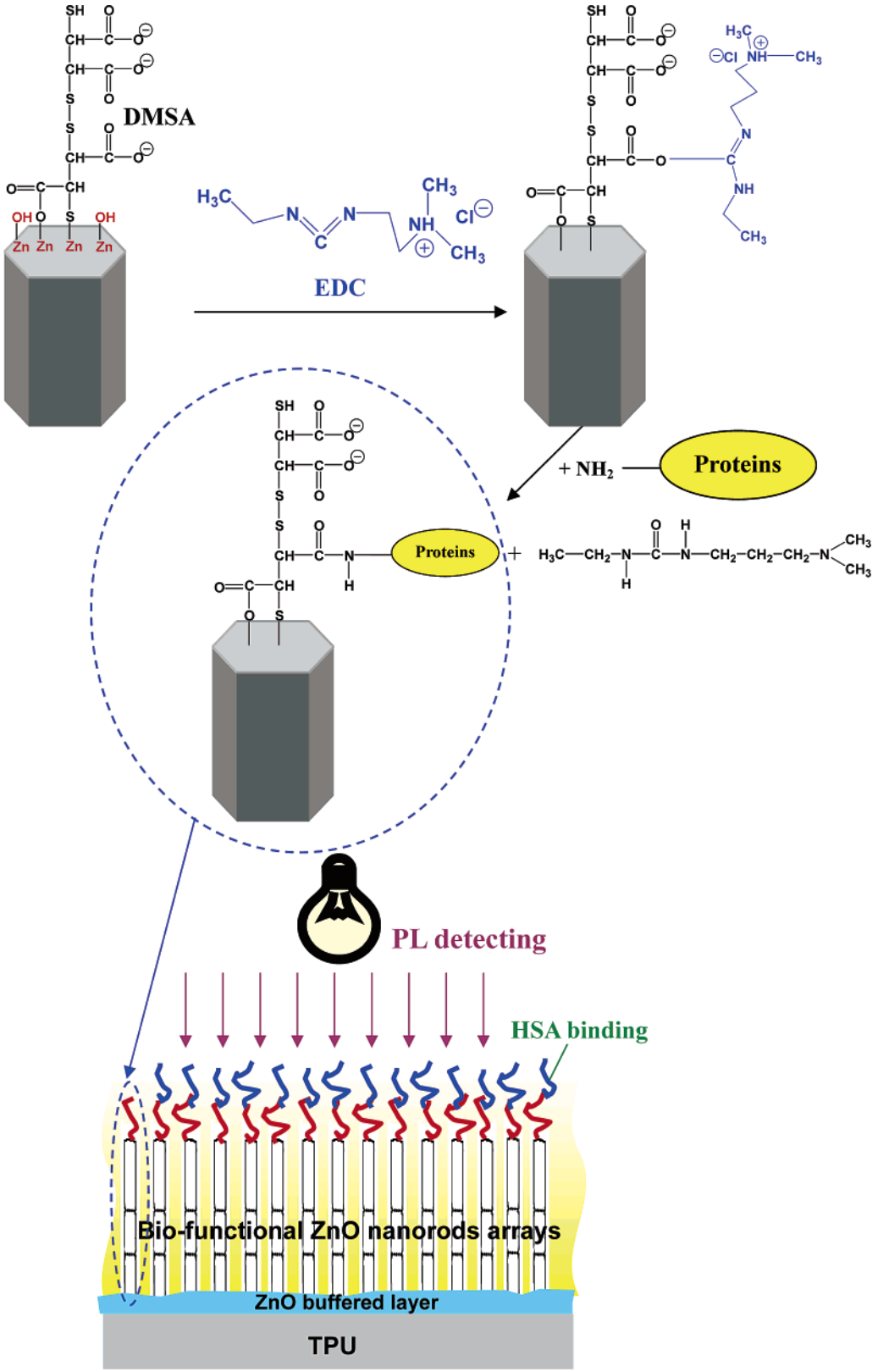

Figure 1. Chemical scheme of DMSA-self-assembled and protein-conjugated ZnO nanorods, and the sensitive optical quality observed by PL detecting while proteins bound.

thioctic acid that is self-assembled onto arrayed ZnO nanorods for sensing applications has not been reported. Moreover, most bioresponses in current biosensors have been detected by dye assay or electrochemical measurement. Few biosensors have been developed using photoluminescence (PL) to detect the changes in the optical properties due to conjugating or adsorbing biomolecules.

Our previous works have demonstrated that arrayed ZnO nanorods can be successfully grown not only on a silicon wafer but also on PC flexible substrates. In this work, TPU was used because it is a common material in biomedical applications and has been approved for in vivo implantation by the Food and Drug Administration (FDA). An in situ process was developed to self-assemble DMSA on arrayed ZnO nanorods grown on

TPU substrate, and then proteins were conjugated on ZnO arrays, which may be applied in biological sensing because of its flexible property and excellent biocompatibility. The characterizations of the biofunctional arrayed ZnO nanorods were investigated by scanning electron microscopy (SEM), X-ray diffraction (XRD), X-ray photoelectron spectroscopy (XPS), contact angle, and dye assay. In addition, being a simple test, the proteins bound to biofunctional ZnO nanorod arrays can be used as a model for biological sensing, and the corresponding PL signals will also be analyzed to detect changes in the optical properties in this paper.

2. Experiment

2.1. Fabrication of Thioctic Acid Self-Assembled ZnO Nanorod Arrays on TPU Substrates. To grow the ZnO nanorods on TPU substrates, a ZnO buffered layer (thickness around 100 nm) was first deposited on the TPU substrates by radio frequency (rf) magnetron sputtering using 99.99% ZnO as the target. After that, the ZnO-coated TPU substrates were first placed in a solution containing an equimolar (0.01 M) aqueous solution of zinc nitrate-6-hydrate [$Zn(NO_3)_2 \cdot 6H_2O$, Riedel-de Haen, Germany] and hexamethylenetetramine (HMT, Sigma, St. Louis, MO) and reacted at 75 °C for 1, 3, and 5 h. Subsequently, DMSA (Aldrich, St. Louis, MO) (0.0005 M) was added into the above three aqueous solutions that had been immersed for 1, 3, and 5 h, respectively (they were designated as 1 h, 3 h, and 5 h addition time), and continued to react at 75 °C until 10 h. For comparison, bare ZnO nanorod arrays were directly grown from the solution (without DMSA) at the same temperature for 10 h. Later, the substrates were removed from the aqueous solutions and rinsed with distilled water three times. Finally, the substrates were dried in a vacuum oven at 50 °C overnight. As expected, the thioctic acid self-assembled ZnO nanorod arrays (ZnO−DMSA) were developed.

2.2. Bioconjugation of Proteins and Binding of Human Serum Albumin (HSA) on ZnO Nanorods. A piece (2×2 cm^2) of TPU film with ZnO−DMSA nanorod arrays was immersed in 20 mL of buffered solution containing 0.01 M EDC (Sigma, St. Louis, MO) in phosphate-buffered saline (PBS, pH = 7.4). After gently shaking (100 rpm) for 24 h at 4 °C, the EDC-activated samples were washed three times with deionized (DI) water.[28,29] Subsequently, the nanorod arrays were immersed in 20 mL of solution containing 10 mg/mL bovine serum albumin (BSA) dissolved in PBS buffer at 4 °C for at least 24 h. The resulting nanorod arrays were washed with PBS buffer five times and subsequently rinsed with DI water five times. The bioconjugated nanorod arrays were designated as ZnO−BSA nanorods. Chemical schemes of the self-assembled DMSA and conjugated BSA of ZnO nanorods are shown in Figure 1.[30−32]

Moreover, the process for HSA (10 mg/mL) bound on ZnO−BSA nanorods was the same as that for BSA conjugated on ZnO−DMSA nanorods. HSA ($-NH_2$) bound onto ZnO−BSA (COOH− groups) nanorods was designated as ZnO−BSA-b-HSA nanorods.

2.3. Grafted Density Determination. The surface density of carboxyl groups (DMSA-COOH) were determined using Toluidine blue O dye (Sigma).[28,29,33] Coomassie brilliant blue G-250 (CBBG, Sigma) protein dye was used to verify the conjugation of BSA on the nanorods surface.[28,29,34] Briefly, a piece of sample (1×1 cm^2) was immersed in 20 mL of 10 mg/dL CBBG solution for 5 h. Thereafter, the sample was extensively rinsed in DI water and allowed to dry. Two pieces of the bare ZnO (control-1) and ZnO-DMSA nanorod (but not activated with EDC, control-2) conjugated proteins were used as the control. The adsorbed dye molecules were desorbed with 20 mL of 10 mg/dL sodium dodecyl sulfate (SDS) solution for 5 h. The absorbance of the dye desorbed was measured at 468 nm using a spectrophotometer, and the surface density of the functional groups was then calculated.

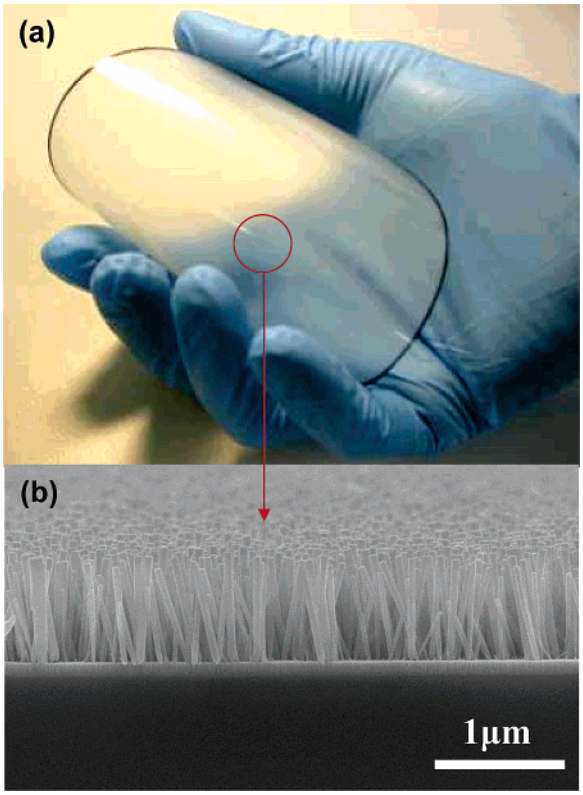

Figure 2. (a) Photograph of ZnO nanorods grown on a flexible 4-in. TPU substrate. (b) SEM image demonstrating that ZnO nanorods with a uniform length are grown on the TPU substrate.

2.4. Characterization Analysis. The morphology of ZnO nanorods was examined by a field-emission scanning electron microscope (FESEM) (JEOL-6500, Japan). The crystal structure was determined using XRD (SIEMENS-D5000, Germany) with Cu Kα radiation. The functional groups on the biofunctional nanorod arrays were analyzed using XPS (ESCALAB 250, Thermo VG Scientific, West Sussex, UK) equipped with Mg Kα at 1253.6 eV at the anode. PL measurement [Kimmon, IK5552R−F, Japan] was performed by the excitation from a 325 nm He−Cd laser (25 mW) at room temperature.

3. Results and Discussion

3.1. Morphology of Arrayed ZnO−DMSA−Protein Nanorods. The photo in Figure 2a shows the densely packed arrays of ZnO nanorods grown on a flexible 4-in. TPU substrate. The SEM cross-sectional images demonstrate that the highly oriented ZnO nanorods with a uniform length of 500−520 nm are perpendicularly grown to the TPU substrate, as shown in Figure 2b. The ZnO nanorods present a well-defined hexagonal shape with a homogeneous diameter of approximately ∼70 nm.

Figure 3 shows the SEM images of bare ZnO, ZnO−DMSA, ZnO−BSA, and the square pattern of ZnO nanorod arrays grown on a TPU surface. It was found that the morphology of the ZnO−DMSA nanorods changes with various DMSA addition times. When DMSA was added at 1 h (Figure 3b), the nanorods appeared to be more circular and larger. When DMSA was added at 3 h, the disordered ZnO nanorods in Figure 3c were observed. However, when DMSA was added at 5 h, it was found that the morphology (shown in Figure 3d) was similar to that of bare ZnO nanorods, shown in Figure 3a. Obviously, the structure change is related to the addition of DMSA, which promotes the

(28) Lin, W. C.; Liu, T. Y.; Yang, M. C. *Biomaterials* **2004**, *25*, 1947.
(29) Liu, T. Y.; Lin, W. C.; Huang, L. Y.; Chen, S. Y.; Yang, M. C.; *Biomaterials* **2005**, *26*, 1437.
(30) Li, W. J.; Shi, E. W. *J. Cryst. Growth* **1999**, *203*, 186.
(31) Yamabi, S.; Imai, H. *J. Mater. Chem.* **2002**, *12*, 3773.
(32) Zhang, J.; Sun, L. *Chem. Mater*. **2002**, *14*, 4172.
(33) Bae, J. S.; Seo, E. J.; Kang, I. K. *Biomaterials* **1999**, *20*, 529.
(34) Kang, I. K.; Kwon, B. K.; Lee, J. H.; Lee, H. B. *Biomaterials* **1993**, *14*, 787.

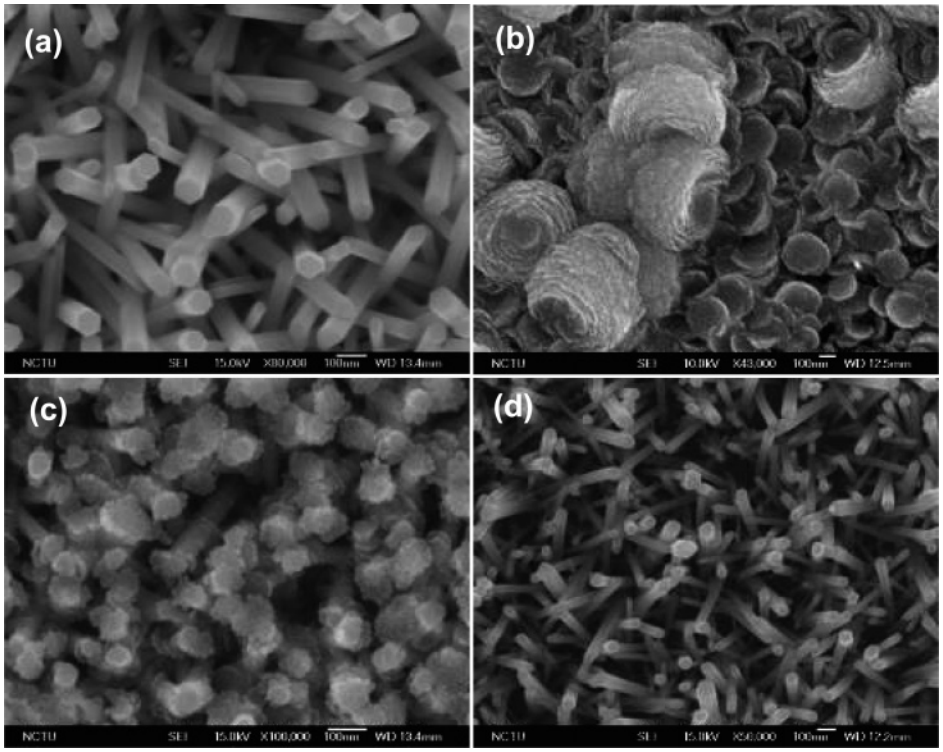

Figure 3. SEM images of (a) bare ZnO, (b) ZnO−DMSA (addition time: 1 h), (c) ZnO−DMSA (addition time: 3 h), and (d) ZnO−DMSA (addition time: 5 h) nanorods.

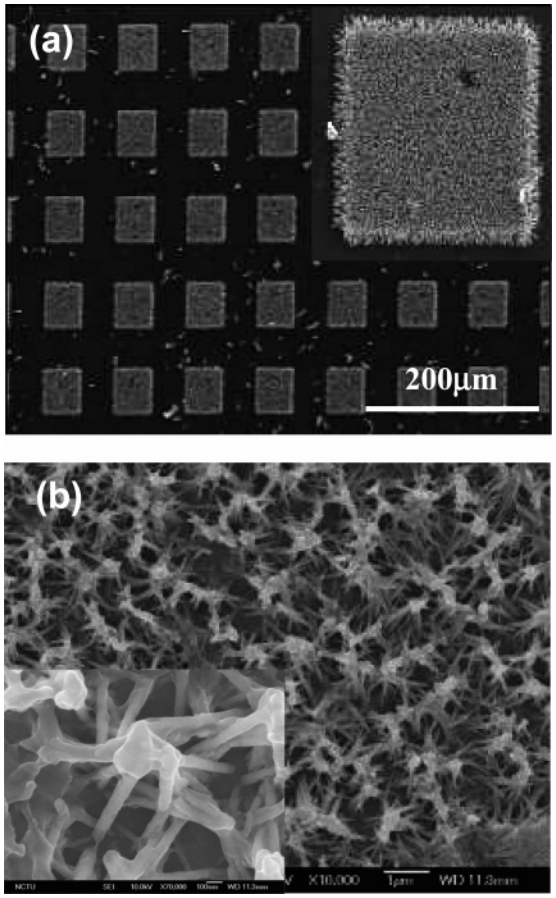

Figure 4. SEM images of (a) the square pattern of arrayed biofunctional nanorods and (b) ZnO−BSA nanorods.

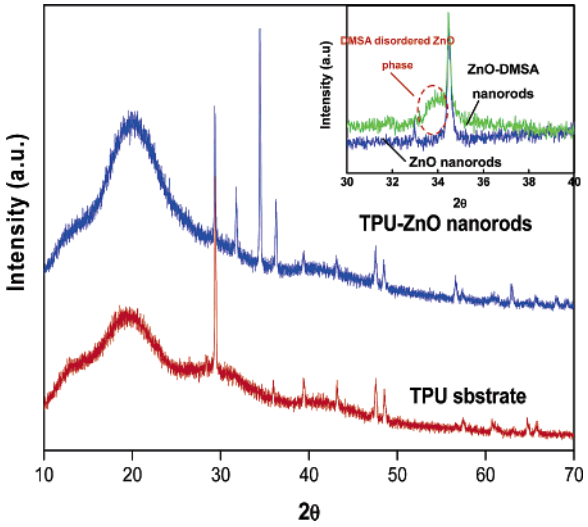

Figure 5. XRD spectra obtained from nanorod arrays of bare ZnO and ZnO−DMSA nanorods grown onto TPU substrates.

dissolution and regrowth of ZnO during the in situ growth process at different DMSA adding times. The mechanism for the ZnO−DMSA composition is very complicated and will be discussed in future works. The more ordered ZnO−DMSA nanorods formed at 5 h addition time were used in this study.

Figure 4a shows the SEM images of large-scale arrayed ZnO nanorods grown on TPU, where the patterned ZnO film on the substrate was fabricated by photolithography and etching processes. Proteins can be conjugated on the ZnO nanorod arrays on the patterned TPU substrates, indicating that the square pattern of the biofunctionalized ZnO nanorod arrays can be used for biosensors. As the BSA proteins were conjugated on the ZnO−DMSA nanorods, it was found that the proteins seemed to congregate a number of ZnO−DMSA nanorods to form mass structures, as shown in Figure 4b.

3.2. Grafted Density Assay. As listed in Table 1, the grafted density of the carboxyl groups on ZnO−DMSA nanorods attained 88.5 nmol/cm^2 by Toluidine blue O dye assay. The carboxyl

Table 1. Surface Density of Arrayed Biofunctional ZnO Nanorod Arrays

	bare ZnO	ZnO−DMSA	ZnO−BSA	control-1[a]	control-2[b]
surface grafting density		88.5 ± 1.8[c]	25.3 ± 1.2[d]	1.3 ± 0.4[d]	3.4 ± 0.8[d]
water contact angle (°)	110.2 ± 2.8	91.6 ± 1.3	71.5 ± 1.5		

[a] Bare ZnO nanorods and then immobilized BSA were used as control-1. [b] DMSA-modified nanorods (but not activated with EDC) and then immobilized BSA were used as control-2. [c] Carboxyl acid (nmol/cm^2), determined with dye staining with Toluidine blue O (for six samples; the second number is the SD). [d] Protein contents (μg/cm^2), determined with CBBG assay (for six samples; the second number is the SD).

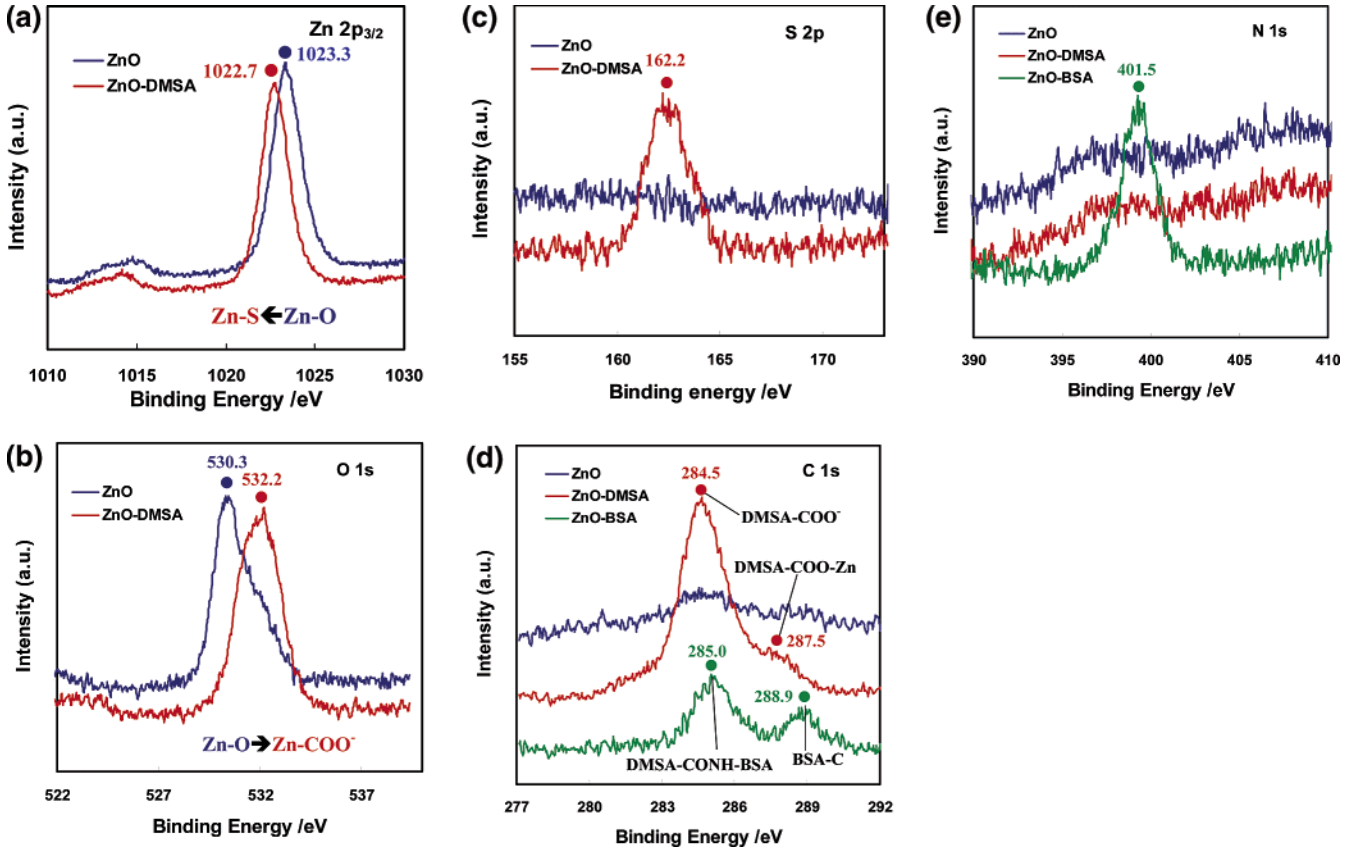

Figure 6. XPS survey scan spectra of arrayed biofunctional ZnO nanorods: (a) $Zn_{2p3/2}$ scan spectra, (b) O_{1s} scan spectra, (c) S_{2p} scan spectra, (d) C_{1s} scan spectra, and (e) N_{1s} scan spectra.

groups of the ZnO−DMSA were then reacted with the amino groups of BSA. The surface immobilizing density of the proteins on the ZnO nanorods by CBBG dye assay was 25.3 μg/cm^2 for BSA.[28,29,34] A similar concept was reported by Kang et al. in which, as poly(methyl methacrylate) (PMMA) films were treated with oxygen plasma, followed by grafting with acrylic acid, the coupled proteins were 13.75 μg/cm^2 for albumin and 7.25 μg/cm^2 for collagen.[34] Moreover, for comparison, the surface immobilizing densities of the proteins of control-1 (1.3 μg/cm^2) and control-2 (3.4 μg/cm^2) were also measured and are shown in Table 1. The results show that very few proteins were bonded to the nanorods. Hence, it could be demonstrated that BSA was effectively chemically bound to the ZnO−DMSA nanorods via EDC activation. In addition, it was also found in Table 1 that the water contact angle decreased when the DMSA was inserted and the proteins were conjugated onto the ZnO nanorods. The higher hydrophilicity in those ZnO nanorod arrays leads to better biocompatibility and hemocompatibility. Hence, these biofunctional ZnO nanorod arrays should be suitable for biomedical applications.

3.3. Surface Characterization Assay. Figure 5 shows the XRD patterns obtained from nanorod arrays of bare ZnO and ZnO−DMSA grown on TPU substrates. A broad 2θ peak for the TPU substrate was found at about 19.8°. After growing ZnO nanorods, the main diffraction peak at 34.4° indexed as the (002) of the wurtzite structure of ZnO appears in the XRD patterns, indicating that ZnO nanorods were grown onto the organic flexible substrates. In addition, comparing the bare ZnO with the ZnO−DMSA nanorods, a broad weak peak starting from 33.2 to 34.2 appears in the ZnO−DMSA nanorods, showing the amorphous-like DMSA-disordered ZnO structure. This suggests that the DMSA has been reacted with the ZnO nanorods.

A comparison of the XPS spectra recorded from the bare ZnO and biofunctional ZnO nanorods is shown in Figure 6. The XPS analysis shows that the biofunctional ZnO nanorods were mainly composed of Zn, O, C, S, and N. Figure 6a shows the XPS data of $Zn_{2p3/2}$ in ZnO and ZnO−DMSA nanorods. The peak in the ZnO-DMSA nanorods was shifted toward a lower binding energy around 0.6 eV (from 1023.3 to 1022.7 eV), implying that some of the Zn−O bonds had been transferred into Zn−S bonds. In Figure 6b, the O_{1s} peak of the ZnO−DMSA nanorods was shifted from 530.3 to 532.2 eV, implying that some of the Zn−O bonds had been transferred into Zn−COO$^-$ bonds. Comparing with the bare ZnO, a S_{2p} peak (binding energy 162.2 eV) was observed in the spectrum of ZnO−DMSA, as indicated in Figure 6c. These results demonstrate that the DMSA is effectively connected to the ZnO nanorods.

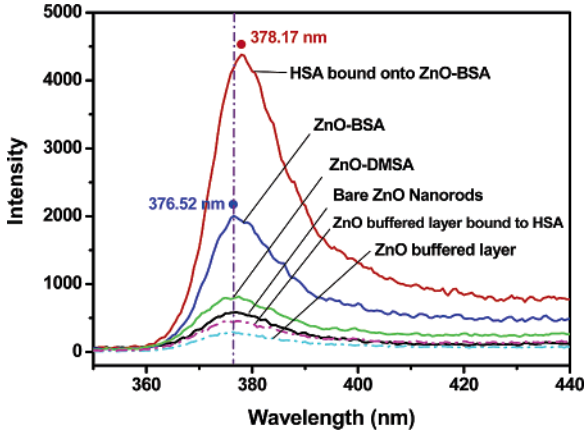

Figure 7. PL detecting of bare ZnO, ZnO−DMSA, ZnO−BSA, and HSA bound onto ZnO−BSA nanorod arrays, as well as that of a ZnO-buffered layer and ZnO-buffered layer-b-HSA as the control.

Furthermore, the C_{1s} peaks of ZnO−DMSA and ZnO−BSA nanorods (284.5 and 285.0 eV, respectively) differed by 0.5 eV, suggesting that DMSA−COO^- bonds transferred into DMSA−CONH−BSA bonds. Moreover, the broad peak (287.3 eV) of DMSA−COO−Zn (Zn−COO^-) bonds in the ZnO−DMSA nanorods and the peak (288.9 eV) of BSA−C bonds in the ZnO−BSA nanorods were also found, but the spectrum of bare ZnO showed no C_{1s} peak, as shown in Figure 6d. In addition, Figure 6e shows the N_{1s} scan spectra of bare ZnO, ZnO−DMSA, and ZnO−BSA nanorods. The NH_2 peak (401−402 eV) can be observed for ZnO−BSA nanorods, but no NH_2 peak can be found for bare ZnO and ZnO−DMSA nanorods. These results again demonstrate that the proteins have indeed been conjugated to the ZnO nanorods.

3.4. Optical Property and Sensitive Characterization. Figure 7 shows the PL intensity of bare ZnO, ZnO−DMSA, ZnO−BSA, and ZnO−BSA-b-HSA nanorods, as well as that of a ZnO-buffered layer (flat-ZnO) and a ZnO-buffered layer bound to HSA (ZnO-buffered layer-b-HSA) as the control. It was found that an enhanced ultraviolet (UV) emission was detected for the ZnO nanorods with the binding of DMSA and BSA. The ZnO−BSA nanorods have a stronger UV emission intensity than the ZnO−DMSA nanorods due to higher grafting density. Furthermore, the UV emission intensity increase is about 2-fold and exhibits a slight red shift (from 376.52 to 378.17) when HSA (grafted density: ∼31.5 $\mu g/cm^2$) was bound to ZnO−BSA nanorod arrays.[28,29,34] The enhanced UV intensity and red shift of these ZnO nanorods in PL might be attributed to both defect passivation and modification on the surface region of ZnO nanorods due to the conjugation of biomolecules. Schvartzman et al.[35] reported similar results on the surface passivation of InP wafers by organic thiols and PI causing enhanced PL intensity.

In addition, a control test found that the ZnO nanorods show more enhanced PL intensity than a flat-ZnO film. In this experiment, a simple trial was made by bonding proteins (HSA) onto a flat-ZnO surface. A weaker PL intensity was detected for the ZnO-buffered layer-b-HSA, which can be attributed to the poor crystallinity of flat-ZnO (ZnO-buffered layer), leading to poor sensitivity. The ZnO nanorods show a significant improvement in sensitive characterization over the flat-ZnO. Therefore, the conjugation of specific biomolecules on the patterned region of arrayed ZnO nanorods can be anticipated to detect the complementary biomolecules on the acceptor side, such as antibody−antigen bioconjugation by PL spectra.

4. Conclusion

In summary, we have successfully developed a process to grow patterned ZnO−DMSA nanorod arrays and then conjugated proteins on flexible substrates (4-in. TPU substrate) at low temperatures. The self-assembly of DMSA (−SH and −COOH) and bioconjugation of BSA (−COOH and $-NH_2$) on the ZnO nanorods could be confirmed by SEM, XRD, EDS, XPS, contact angle, PL spectra, and dye assay. While proteins were bound onto the biofunctional ZnO nanorod arrays, the optical properties were changed, as detected by PL spectra. Furthermore, the ZnO nanorods showed a significant improvement in sensitive characterization over the flat-ZnO. These results demonstrate that this simple and low-cost process provides a promising route for sensing to detect protein conjugation.

Acknowledgment. The authors gratefully acknowledge the financial support of the National Science Council of Taiwan through Contract No. NSC-93-2216-E-009-005.

LA052363O

(35) Schvartzman, M.; Sidorov, V.; Ritter, D.; Paz, Y. *Semicond. Sci. Technol.* **2001**, *16*, 68.